Enhancement of Photocatalytic Cancer Cell-Killing Activity by Using Ag@TiO_2 Core-Shell Composite Nanoclusters

Md. Abdulla-Al-Mamun, Hailong Yang, Bashir Ahmmad and Yoshihumi Kusumoto*

Kagoshima University, Faculty of Science
Department of Chemistry and Bioscience, 1-21-35 Korimoto,
Kagoshima 890-0065, Japan,
Phone & Fax: +81-99-285-8914, E-mail: kusumoto@sci.kagoshima-u.ac.jp

ABSTRACT

The photocatalytic cancer cell-killing activity of the Ag metal core-TiO_2 shell (Ag@TiO_2) composite colloidal nanoclusters has been investigated on HeLa cells under the UV-visible light irradiation. The Ag@TiO_2 composite nanocluster photocatalyst with the uniform size and shape was successfully synthesized by a simple citrate reduction method. The photocatalytic cell-killing activity of the Ag@TiO_2 nanoclusters was found to vary with the molar ratio of Ag to TiO_2. The direct involvement of the metal particles in mediating the electron transfer from the photoexcited TiO_2 under the band gap excitation is considered to carry out the efficient photocatalytic reaction on the cells. The charge separation and the interfacial charge-transfer promote the photocatalytic cancer-cell killing more than the TiO_2 semiconductor alone. It was found that the Ag@TiO_2 nanoclusters under the low concentrations kill HeLa cells by 100%, whereas TiO_2 nanoparticles alone kill only ca. 25% under the same concentrations.

Keywords: citrate reduction, Ag core–TiO_2 shell, composite nanoclusters, photocatalysis, cancer cell killing.

1 INTRODUCTION

The unique oxidation and reduction properties of semiconductor are providing a potential means for the photocatalytic malignant cells killing.

When a semiconductor (e.g. TiO_2) absorbs the photons with energy greater than its band gap, the electrons from its valance band are excited to its conduction band. Removal of an electron from the valance band creates a positively charged vacancy, called a positive hole, in the valance band. These electrons and holes in single component semiconductor nanoparticles exhibit relatively poor photocatalytic efficiency (<5%) and the majority of the photogenerated charge carriers undergo recombination [1-2].The conduction band electrons must be removed rapidly from TiO_2 to prevent the recombination with the holes and allow the successful charge separation for enhancing the photocatalytic activity. The photocatalytic oxidation and reduction of semiconductor TiO_2 are strongly enhanced by contact with noble metal nanoparticles.

Metal nanoparticles deposited to TiO_2 nanostructures undergo Fermi level equilibration following the UV-excitation and enhance the efficiency of the charge-transfer process [3-4]. Charge recombination or the grain boundary of heterogeneous semiconductor often limits the efficiency of light energy conversion. The semiconductor-metal composites system is able to suppress the charge recombination to enhance the energy conversion efficiency [5].

In the semiconductor-metal nanocluster system, the metal nanoparticles are dispersed on oxide surface. The photogenered electrons of TiO_2 are capable to reduce the metal nanoparticles that depend on reactants and surrounding media. Corrosion or dissolution of the noble metal particles during the photocatalytic reaction is likely to limit the use of noble metal such as Ag and Au [6-8]. A better synthetic design can significantly improve the catalytic performance of metal-oxide composites. Hirakawa et al. [9] found that the photocatalytic properties, such as photoinduced charge separation, band gap excitation and charge equilibrium in Fermi level as well as core-shell structure, of the metal core/outer shell TiO_2, make itself a superior photocatalyst.

Generally Ag nanoparticles are chemically very reactive, can be oxidized at direct contact with TiO_2 and can produce silver oxide (AgO). To prevent the oxidation of Ag we introduce the very simple new method to prepare the Ag@TiO_2 by citrate reduction which can cap the Ag nanoparticles and reduce them rapidly at boiling temperature of iso-propanol. Our point of view is that if the solutions have no Ag^+ ion, it can not react with dissolved O_2.

Metal/semiconductor colloidal nanoparticles are known to be the potential materials that selectively destroy malignant cells. Nanoparticles, smaller than 20 nm, can move out of a blood vessel as they circulate through the body [10]. The smaller particles which are more soluble in hydrophobic or nonpolar oil diffuse more rapidly across the lipid bilayer by passive diffusion [11-12]. The pore size of the blood vessel endothelium wall of a normal cell is ca. 10 nm while that of a cancer cell is 10-100 nm [13-14]. The anatomical difference in the structure of blood vessel

endothelia near the cancer and the normal cells makes the size-tunable nanoparticles / nanocomposite feasible to reach selectively on the surface of cancer cells as shown in Fig 1 [15-16]. Moreover, TiO_2 particles were adsorbed on the cell membrane and phagocytized into the cytoplasm during 24-h incubation with the cells reported elsewhere [17].

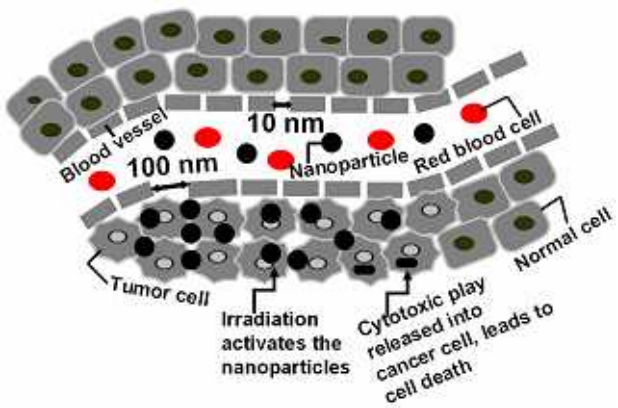

Fig. 1: A simplified representation of the nanoparticles entering the cancer cells and the release of their cytotoxic action when irradiated by external energy.

Ag@TiO_2 has been successfully used to enhance the photocatalytic decomposition of organic compounds and photokilling of bacteria [18-20]. The enhanced photocatalytic activity in cancer cell (HeLa) killing due to the plasmon excited metal nanoparticles and excitation of photogenerated electron-hole pairs in TiO_2 has never been reported to the best of our knowledge. Here we report the photocatalytic effect of Ag@TiO_2 on cancer cells in several concentrations and also in different molar ratios of Ag to TiO_2 nanoclusters. We found that the photocatalytic cancer cell killing by Ag@TiO_2 required only one forth of irradiation time compared to TiO_2 and the cancer cell killing efficiency by Ag@TiO_2 was 75% higher than that of TiO_2 alone in the same concentration.

2 EXPERIMENTAL

2.1 Chemicals and Materials

Titanium (IV) (triethanolaminato)-isopropoxide ($N((CH_2)_2O)_3TiOCH(CH_3)_2$) (TTEAIP) (80 wt % solution in 2-propanol) was purchased from Aldrich and $AgNO_3$ (99.8%) and Sodium citratre (99.0%) were purchased from Wako pure chemical industries, Ltd. TiO_2 (Degussa, P25) was used with a mainly anatase structure (ca. 80%) under the shape of non-porous polyhedral particles of ca. 20 nm mean size with surface area of 49.9 m^2/g.

2.2 Synthesis of Ag@TiO_2 Core-shell Nanocluster Photocatalyst

The Ag@TiO_2 core-shell nanocluster was prepared from $AgNO_3$ and TTEAIP. $AgNO_3$ and TTEAIP were used as sources of Ag and TiO_2, respectively. Five different suspensions of Ag@TiO_2 nanoclusters were prepared by keeping the $AgNO_3$ concentration constant at 1mM while varying the TTEAIP concentration at 1,3,5,7 and 9 mM. These five Ag/TiO_2 suspensions contained [Ag]:[TiO_2] ratios of 1:1, 1:3, 1:5, 1:7 and 1:9, respectively. All the concentrations are based on molar concentrations.

2.3 Instrumental Analysis

Absorption spectra were recorded on a UV-visible spectrophotometer (Shimadzu Corporation, MPS-2000, Kyoto, Japan) in a 1 cm pathlength quartz cuvette solution. The size and shape of the nanocluster is analyzed by transmission electron microscopy (TEM) using a JEOL JEM-3010 VII TEM operating at 300 kV. The nanocluster surface condition was also analyzed by field-emission scanning electron microscope (FE-SEM, Hitachi, S-4100H) and X-ray photoelectron spectroscopy (XPS, Quantum-2000, Scanning ESCA-1000 microprobe with Magnesium α radiation, Shimadzu) analyzer.

2.4 Cell Culture and Cellular Incubation with Colloidal Nanoclusters

2.4.1 Cell line and counting method

A typical cancer cell line, human cervix epitheloid carcinoma (HeLa), was used in this study. The cells were cultured in minimum essential medium (MEM, Sigma) plus 10% new born calf serum (NBS, Invitrogen Corporation, Gibco) at 37 °C under 5% CO_2. The cells were plated at a concentration of about $3x10^5$ cells in 60-mm Petri dishes and were allowed to grow for 3 days. The old culture medium was replaced with nanocluster colloidal solution and recultured for 24 h in an incubator. The colloidal solution was removed and washed with phosphate buffer saline (PBS, Invitrogen Corporation, Gibco). After the cells were cleaved by trypsin-EDTA (Gibco) and cells were stained with trypan blue (Nacalai Tesque, Inc, Kyoto, Japan). Then, the cells were counted under magnification x10 in a bright field microscope. The cell survival was determined as the percentage of the number of unstained (live) cells against the control dish cells.

2.4.2 Light irradiation of colloidal nanoclusters on cells.

In photocatalytic experiments, a continuous wavelength from a Xenon CX-04E lamp (Inotech, Japan) was used. The light wavelength over 350-600 nm was selected using a band pass filter (V-B46, Asahi Techno Glass) together with a heat cut-off filter. The light power was measured by using a spectroradiometer (Model LS-100, EKO Instruments Co.

Ltd.). The maximum power of light was 100W and irradiation time was 5 min for each dish. The cells were cultured for 3 days and then the medium was replaced with colloidal nanocluster solution, and again incubated for 24 h. All the dishes were exposed to light with different amounts of colloidal nanocluster solution whereas only one dish was exposed to light without nanocluster solution (light control dish). The colloidal solution was removed and washed with PBS and then stained with trypan blue to test the cell viability by counting. The dead cells accumulated the dye and were stained blue color while living cells have no color. The living cells were counted and estimated as the percentage of the number of the cells against the control dish cells.

2.4.3 Cells imaging method

The images were taken using an inverted Olympus CKX41 microscope with a numerical light field condenser (N.A.0.3), which delivers a very narrow beam of white light from tungsten lamp (6V30W halogen illumination) on top of the sample. A 40x / 0.55 Php objective was used to collect only the scattered light from the samples. The light field pictures were taken using an Olympus digital camera (Model No. C-5060, wide zoom).

3 RESULTS AND DISCUSSION

3.1 Absorption Spectral Analysis

The UV-visible absorption spectra of $Ag@TiO_2$ nanocluster suspensions show the strong absorption in the visible region with plasmonic peaks [Fig.2]. The plasmonic peaks indicate that the Ag core is not oxidized [21].

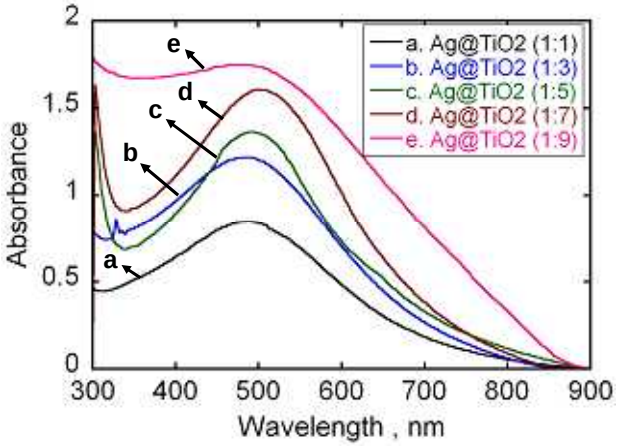

Fig. 2: Absorption spectra of various $Ag@TiO_2$ nanoclusters.

The lower ratios of the TiO_2 shell to the Ag core resulted in dampening and broadening of the surface plasmon band (Fig.2, spectra (a) and (b)) and at higher ratios of the TiO_2 shell the plasmon band of Ag core becomes obscure (Fig.2 (e)). It is interesting to note that an increase in the concentration of the precursor of TiO_2 leads to an increase in the shell thickness. The result (Fig.2) indicates that by increasing the TiO_2 shell thickness, the plasmon absorption bands of $Ag@TiO_2$ increase up to the optimum level and then gradually decreases due to an increase in the shell thickness of TiO_2 around the Ag core. We found the optimized shell thickness with uniform covering of $Ag@TiO_2$ at 1:5 and 1:7 molar ratios.

3.2 TEM Analysis of $Ag@TiO_2$

The TEM images show that the size and shape of $Ag@TiO_2$ nanoparticles are mostly spherical and symmetrical [Fig.3(a)]. The round dark structure of TiO_2 shell around the Ag core clearly shows that the core is uniformly covered by the shell [Fig. 3(b)].

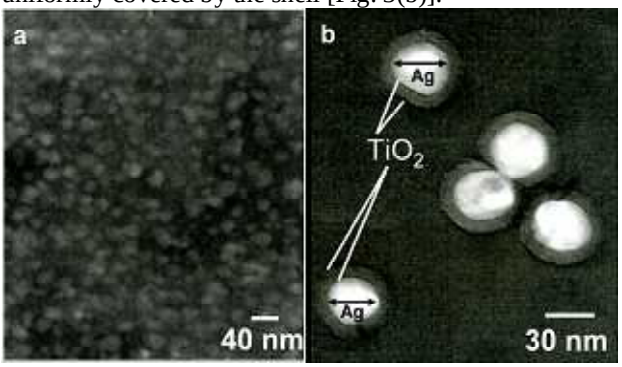

Fig. 3: TEM images of $Ag@TiO_2$. (a) Ag is uniformly covered by TiO_2 layer. (b) The well crystalline nature of metallic core and the uniform shell thickness of TiO_2 are shown.

These core-shell composite nanoclusters are mostly spherical and overall diameters were 20-40 nm. All Ag core particles have an uniform thin capping of TiO_2 and the shell thickness is in the range of about 3-5 nm.

3.3 FE-SEM and XPS Analysis

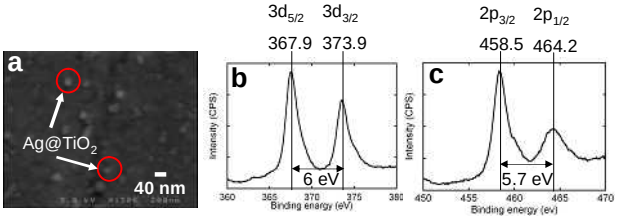

Fig. 4: (a) FE-SEM image of the $Ag@TiO_2$ nanocluster morphology. The X-ray photoelectron spectroscopic scan survey in the region of (b) Ag 3d (c) Ti 2p of the as-prepared $Ag@TiO_2$ nanocluster

The FE-SEM image of the $Ag@TiO_2$ composite nanocluster shows that Ag is covered with the TiO_2 nanocluster and the particle diameter is about 30 nm. The presence of metallic Ag core was confirmed by the X-ray

photocelectron spectroscopy (XPS) analysis. The peaks $3d_{3/2}$ and $3d_{5/2}$ observed at 373.9 and 367.9 eV were ascribed to the metallic silver (Fig.4(b)). The XPS-analysis result of TiO_2 is shown in Fig. 4(c). The peaks located at 464.2 and 458.5 eV are assigned to Ti $2p_{1/2}$ and Ti $2p_{3/2}$, respectively. The splitting width between Ti $2p_{1/2}$ and Ti $2p_{3/2}$ is 5.7 eV, indicating a normal state of Ti^{4+} in as-prepared mesoporous TiO_2 [22].

3.4 Photocatalytic Cancer Cell Killing Enhancement Using Ag@TiO_2 Nanoclusters

The cell dishes were incubated with different amounts of MEM containing Ag@TiO_2 nanocluster solutions (4, 8, 12, 16 and 20 μl) and another dish without nanocluster solution (controlled dish) was also incubated [Fig.5]. Under 5-min light irradiation, 100% cells were killed in the presence of 20 μl Ag@TiO_2 (1:5 and 1:9) nanoclusters colloid [Fig.5].

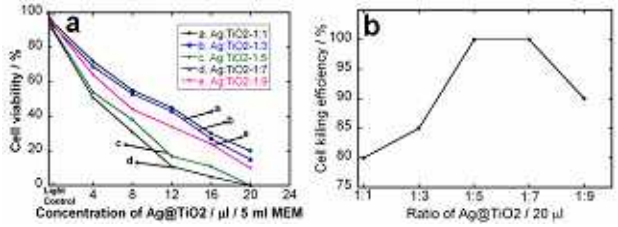

Fig. 5: Surviving fractions of HeLa cells in the presence of Ag@TiO_2 nanoclusters colloid. (a) Cell viability in different ratios of Ag:TiO_2. (b) 100% cells were killed at 1:5 and 1:7 ratios of Ag:TiO_2 in the presence of 20 μl Ag@TiO_2 colloid.

4 CONCLUSION

We introduced the new simple method to prepare the Ag@TiO_2 core-shell composite nanoclusters. We proved that the Ag core is in the metallic state and is uniformly covered with the TiO_2 shell, determined by XPS and TEM analyses. The Ag@TiO_2 core-shell nanoclusters were found to increase the efficiency of interfacial charge-transfer as well as to increase the photocatalytic activity on the cancer (HeLa) cell killing.

REFERENCES

[1] P. V. Kamat, Chem. Rev.93, 267, 1993.
[2] A. L. Linsebigler, G. Lu, J. T. Jr. Yates, Chem. Rev, 95, 735, 1995.
[3] M. Jakob, H. Levanon, P. V. Kamat, Nano Lett, 3, 353, 2003.
[4] V. Subramanian, E. E. Wolf, P. V. Kamat, J. Am. Chem. Soc., 124, 4943, 2004.
[5] P. V. Kamat, J. Phys. Chem. B, 106, 7729, 2002.
[6] V. Subramanian, E. Wolf, P. V. Kamat, J. Phys. Chem. B,105, 11439, 2001.
[7] V. Subramanian, E. E. Wolf, P. V. Kamat, Langmuir,19, 469, 2003.
[8] D. Lahiri, V. Subramanian, T. Shibata; E. E. Wolf, B. A. Bunker, P. V. Kamat, J. Appl. Phys., 93, 2575, 2003.
[9] T. Hirakawa, P. V. Kamat, J. Am. Chem. Soc., 127, 3928, 2005.
[10] S. E. McNeil, Journal of Leukocyte Biology, 78, 585, 2005.
[11] B. Alberts, A. Johnson, J. Lewis, M. Raff, K. Roberts and P. Walter, Molecular biology of the cell, 4th ed., 616-619, 2002.
[12] I. Brigger, C. Dubernet and P. Couvreur, Advance Drug Delivery Reviews, 54, 631, 2002.
[13] Y. Matsumura and H. Maeda, Cancer Research, 46, 6387, 1986.
[14] D. R. Siwak, A. M. Tari and G. Lopez- Berestein, Clinical Cancer Research, 8, 955, 2002.
[15] N. Kohler, C. Sun, J. Wang and M. Zhan, Langmuir, 21, 8858, 2005.
[16] B. D. Chithrani, A. A. Ghazani and W.C.W. Chan, Nano Letts., 6, 662, 2006.
[17] R. Cai, K. Hashimoto, K. Itoh, Y. Kubota, A. Fujishima, Bull. Chem. Soc. Jpn., 64, 1268, 1991.
[18] Mohammad R. Elahifard, S. Rahimnejad, S. Haghighi, Mohammad R. Gholami, J. Am. Chem. Soc., 129, 9552, 2007.
[19] Y. Liu, X. Wang, F. Yang, X. Yang, Microporous and Mesoporous Materials, 114, 431, 2008.
[20] C. Hu, Y. Lan, J. Qu, X. Hu, A. Wang, J. Phys. Chem. B, 110, 4066, 2006.
[21] K. Awazu, M. Fujimaki, C. Rockstuhl, J. Tominaga, H. Murakami, Y. Ohki, N. Yoshida and T. Watanabe, J. Am. Chem. Soc., 130, 1676, 2008.
[22] C.D. Wagner, W.M. Riggs, L.E. Davis, J.F. Moulder, Hand Book of X-ray Photoelectron Spectroscopy, pp. 112 and 68, 1979.